J E M T
Journal of Earth and Marine Technology
homepage URL: ejurnal.itats.ac.id/jemt

The Effect of Stress Distribution Around the Decline Shaft on The Support System Stability in Underground Mining

Diana Irmawati Pradani [1]
[1] Department of Civil Engineering, Politeknik Negeri Malang
e-mail: dianapradani@polinema.ac.id
DOI: j.jemt.2021.v2i1.1726

Article info
Received:
February 18, 2021
Revised:
February 28, 2021
Accepted:
March 6, 2021
Published:
March 31, 2021

Keywords:
Decline shaft, stress distribution

Abstract
The decline shaft is one of the main facilities in an underground mining work that is used as access to the mining panel from the surface. Making decline shafts on materials with weak characteristics is one of the important geotechnical issues that must be considered. The initial stage of making decline shaft holes is carried out on a relatively shallow ground surface or soil depth so that the horizontal stress that works is greater than the vertical stress. This excavation process will change the direction and magnitude of the initial stress from being in an equilibrium state to being disturbed. In addition to the stress on the rock mass, the condition of weak soil strength will affect the behavior and distribution of stresses working around the decline shaft hole. If the stress around the decline shaft exceeds the strength of the rock, there will be instability in the decline shaft so that strength is needed to control the existing stress.

1. Introduction

In general, the decline shaft hole is the main access used to go to the mining panel. In addition to being a link between the surface of the ground (surface) and the mining panel, other functions are the decline shaft as access for exploration activities, haul roads (humans, tools, waste, and ore), ventilation routes, and drain networks. In the process of making the decline shaft holes will disturb the natural stresses that exist in the rock mass. During the excavation of the rock mass, the stress conditions will change dramatically because the rock that was subjected to initial stress and after excavating the surrounding stress will be redistributed [1]–[4]. A basic understanding of the magnitude and direction of in-situ stress and induced stress is very important in the process of making incline shaft holes. In several cases that occurred when the incline shaft was excavated, the stress exceeds the strength of the rock and causes instability in the decline shaft [5]. This will affect the determination of the type of support that will be used and in terms of safety and security of the incline shaft holes. The coal as the rock subject distribution depends on the coal quality that related to the coal formation [6], the underground design also related to the dewatering system [7] and ventilation system [8], at least all of the aspects will contribute to the economical activity [9].

The in situ stress at a point is determined by the loading conditions of the material above it as a result of previous geological processes. Changes in in-situ stress conditions can be caused by several things, including changes in temperature and chemical processes such as leaching, evaporation, and mineral recrystallization. Complex and heterogeneous stress conditions are generated by mechanical processes such as the formation of fractures, shifts between the fracture planes, and the viscous-plastic flow in the material. Some of the factors that influence the in-situ stress conditions according to Brady and Brown (1985) [10] are:

1. Surface Topography
2. Erosion
3. Residual Stress
4. Inclusion
5. Tectonic Activity [11]

6. Field of Discontinuity

In civil and mining construction works, the determination of the location for making an opening is based on the direction of the regional principal stress. Measurements of vertical in-situ stress across several mines and civil works indicate that this relationship is quite valid despite the considerable spread of data. A simple method that can be used to determine the stress state in the rock mass without in-situ measurements is to assume that the vertical stress (σv) on the rock mass at a certain depth is equal to the weight per unit area of the rock above it or:

$$\sigma = \rho\, g\, h \quad \text{.....(1)}$$

where,
σ: vertical in-situ stress (Kg/cm^2)
ρ: weight of rock contents (ton/m^3)
g: acceleration due to gravity (m/s^2)
h: depth (m)

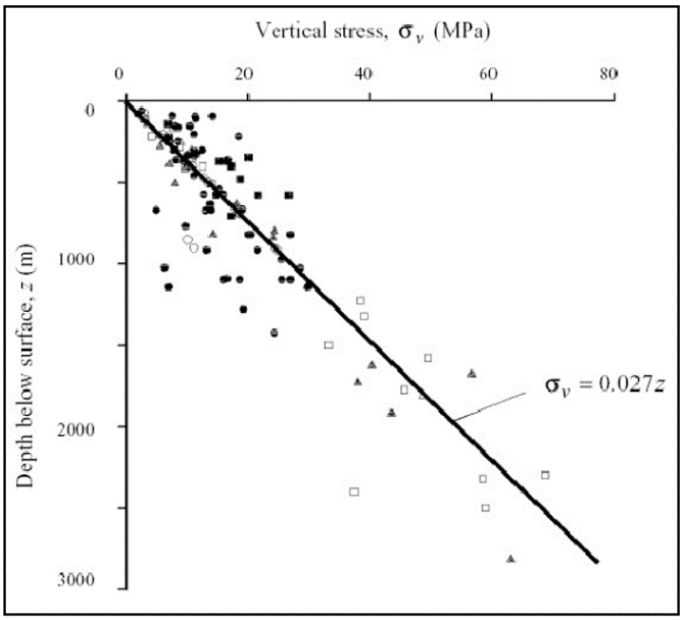

Figure 1. Relationship between Vertical In Situ Stress and Depth (modified from [12])

The simple hypothesis used in predicting the state of two horizontal in-situ stresses is the homogeneity, isotropy, and rheological behavior of the rock mass. Horizontal in situ stress is more difficult to predict and perform than vertical in situ stress. In some cases with very large depths (h), the horizontal in-situ stress becomes hydrostatic or litho-static, ie k = 1 and σh = σv. The empirical approach that has been taken by several previous researchers ([13], [14]) in several mining works and civil projects shows that k values tend to be high at shallow depths and decrease with increasing depth. In addition, [15] stated that for gravity loads where there is no lateral strain, the value of k does not depend on the depth expressed as:

$$k = \frac{\upsilon}{1-\upsilon} \quad \text{.....(2)}$$

Where,
υ: poisson ratio rock mass
σ_h: k σ_v

The analytical calculation of the in-situ stress shows that using this approach the horizontal in-situ stress value will always be less than the vertical in-situ stress. The reality in the field by conducting direct measurements of horizontal in-situ stress shows that the stress value is not always smaller than the vertical in-situ stress. This approach has proven invalid and is rarely reused, [16] proposes the following equation:

$$k = 0.25 + 7\,E_h(0.001 + \frac{1}{z}) \quad \text{.....(3)}$$

where,

E_h: modulus deformation (GPa)

z : depth (m)

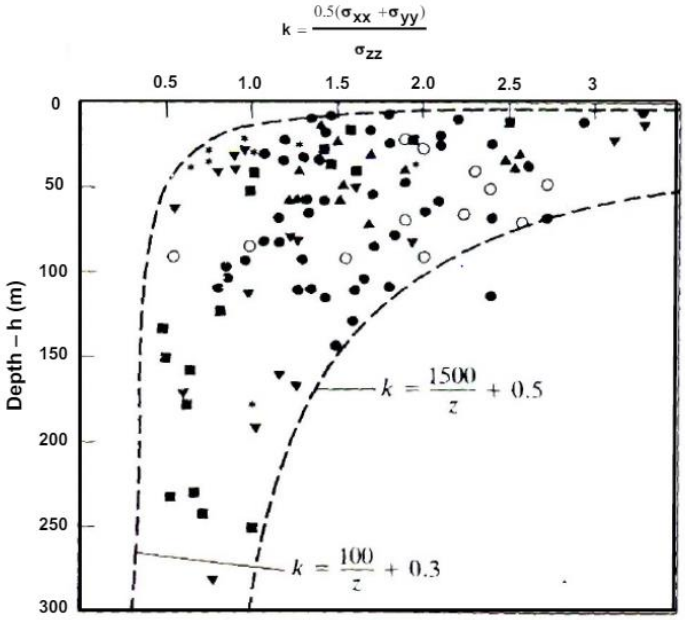

Figure 2. Comparison of Average Horizontal In-Situ Stresses to Vertical In-Situ Stresses [12]

Before excavation, the rock mass is in a state of equilibrium and after excavation, the equilibrium is disturbed and can change the initial stress distribution. When an opening is made in the rock mass, the unexplored rock receives a greater load than it did before it was excavated. The initial voltage will change to the induced voltage. The stress distribution around the opening can be calculated using the Kirsch (1898) equation. [17] derived the equations for radial stress (σr), tangential stress (σθ), and shear stress (τrθ) around a tunnel with a circular cross-section.

$$\sigma_r = \left[\left(\frac{\sigma_v + \sigma_h}{2}\right)\left(1 - \frac{R^2}{r^2}\right)\right] + \left[\left(\frac{\sigma_v - \sigma_h}{2}\right)\left(1 - \frac{4R^2}{r^2} + \frac{3R^4}{r^4}\right) cos2\Theta\right] \quad \text{.....(4)}$$

$$\sigma_\Theta = \left[\left(\frac{\sigma_v + \sigma_h}{2}\right)\left(1 - \frac{R^2}{r^2}\right)\right] + \left[\left(\frac{\sigma_v - \sigma_h}{2}\right)\left(1 + \frac{3R^4}{r^4}\right) cos2\Theta\right] \quad \text{.....(5)}$$

$$\sigma_{r\Theta} = \left[-\left(\frac{\sigma_v - \sigma_h}{2}\right)\left(1 + \frac{2R^2}{r^2} - \frac{3R^4}{r^4}\right) sin2\Theta\right] \quad \text{.....(6)}$$

where,

στ: radial stress

σθ: tangential stress

σrθ: shear stress

σv: vertical stress

σh: horizontal stress

θ: the angle formed to the point of observation clockwise

R: the radius of the opening

R: distance from the center of the opening hole to the point of observation

Determination of plastic zone and deformation at

$$\frac{d_p}{d_o} = \left(1.25 - 0.625\,\frac{p_i}{p_o}\right)\frac{\sigma_{cm}}{p_o}^{\left(\frac{p_i}{p_o} - 0.57\right)} \quad \text{.....(7)}$$

$$\frac{\delta_i}{d_o} = \left(0.002 - 0.0025\,\frac{p_i}{p_o}\right)\frac{\sigma_{cm}}{p_0}^{\left(2.4\frac{p_i}{p_o} - 2\right)} \quad \text{.....(8)}$$

where,

dp: radius of plastic zone
δi: tunnel sidewall deformation
do: original tunnel radius
pi: internal support pressure
po: horizontal stress
θ: in situ stress
σcm: rock mass strength

2. Methodology

Making decline shaft is done on claystone rock with a weak category. The decline shaft is the main entrance which will be made with a slope of 140 to penetrate the coal seam from the surface. The geometry of the incline shaft has a 6 m wide and 5 m high horseshoe shape (Figure 3).

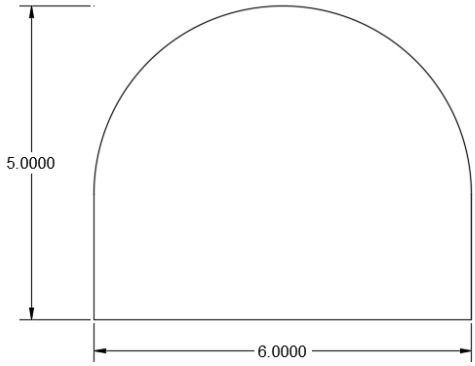

Figure 3. Decline Shaft Geometry (Front View)

The rock mass category of claystone material is obtained from the calculation of the Rock Mass Rating [18] using five main parameters, namely: rock strength value, RQD, fracture space, fracture conditions, and groundwater conditions. From these five parameters, the RMR value of claystone used in making incline shaft holes ranges from 33 - 51 and is included in the bad-medium rock mass class. The value of the Q-System is 0.19 - 2.18, which is included in the very poor-poor rock class.

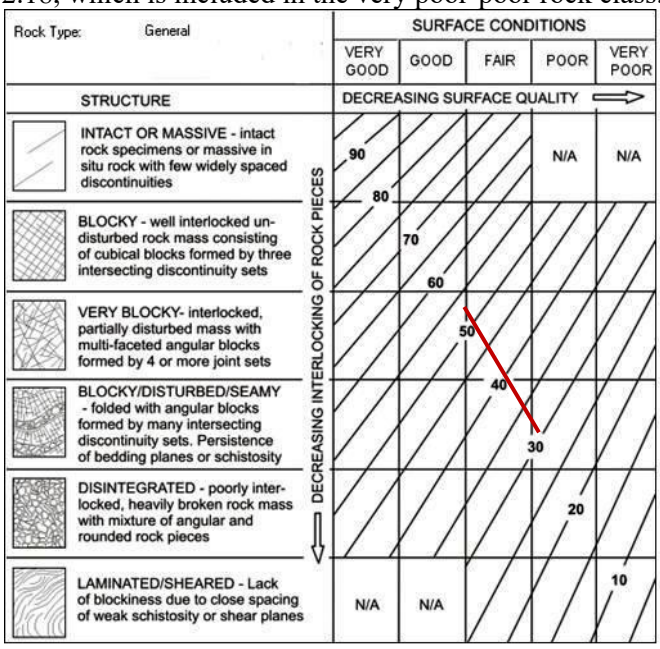

Figure 4. Value of Geological Strength Index for Claystone Rocks [12]

Testing claystone samples obtained the value of material properties used in the numerical two-dimensional analysis. The numerical two-dimensional analysis process uses the RS2 program (Phase2, Rocscience). This calculation uses the finite element method which can be used for various types of soil and rock. The properties of the claystone material used in the analysis process are shown in Table 1.

Table 1. Claystone Material Properties

Claystone		
Unit Weight	MN/m3	0.025
Poisson's Ratio		0.28
E	MPa	4113.79
Tensile Strength	MPa	0.64
Fric. Angle	deg	24.67
Cohesion	MPa	1.27

3. Results

From the results of 2D numerical calculations using the finite element method, the values of sigma one and sigma three are obtained as shown in Figure 5, Figure 6, and Figure 7.

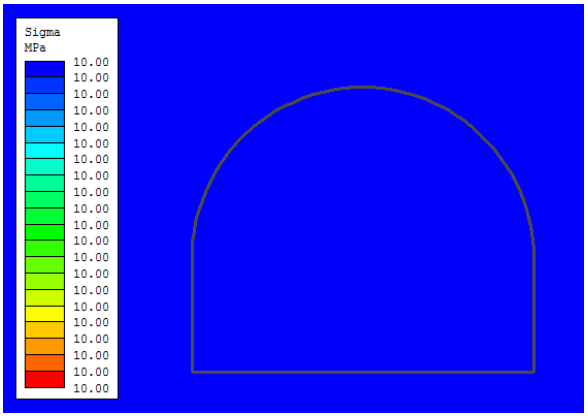

Figure 5. Value Stress at the Decline Shaft Before Excavation

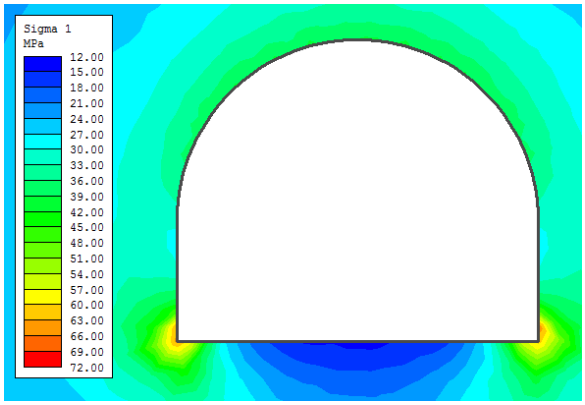

Figure 6. Value Sigma One on the Decline Shaft

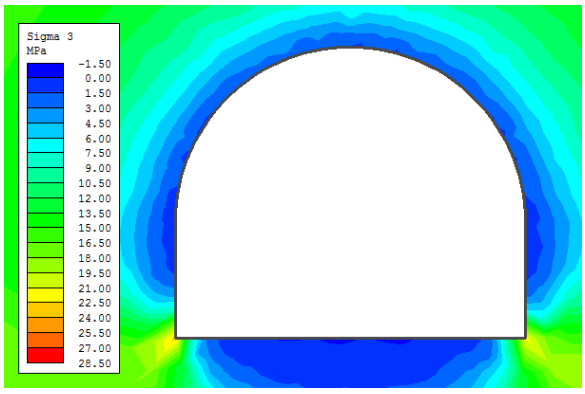

Figure 7. Value Sigma Three on the Decline Shaft

The above analysis can be seen from the stress value in the decline shaft before excavation is carried out, in a stable and equilibrium state. During the excavation of claystone rock, the stress condition around the decline shaft, which initially has evenly distributed stress, is then redistributed [19]. Rocks around the decline shaft that are not excavated will receive a greater load because the part that should receive the load has been disturbed (Figure 8). This results in induced stress. The horizontal stress value increases when approaching the face decline shaft. The further away from the face the stress value decreases and approaches the rock mass stress value [17].

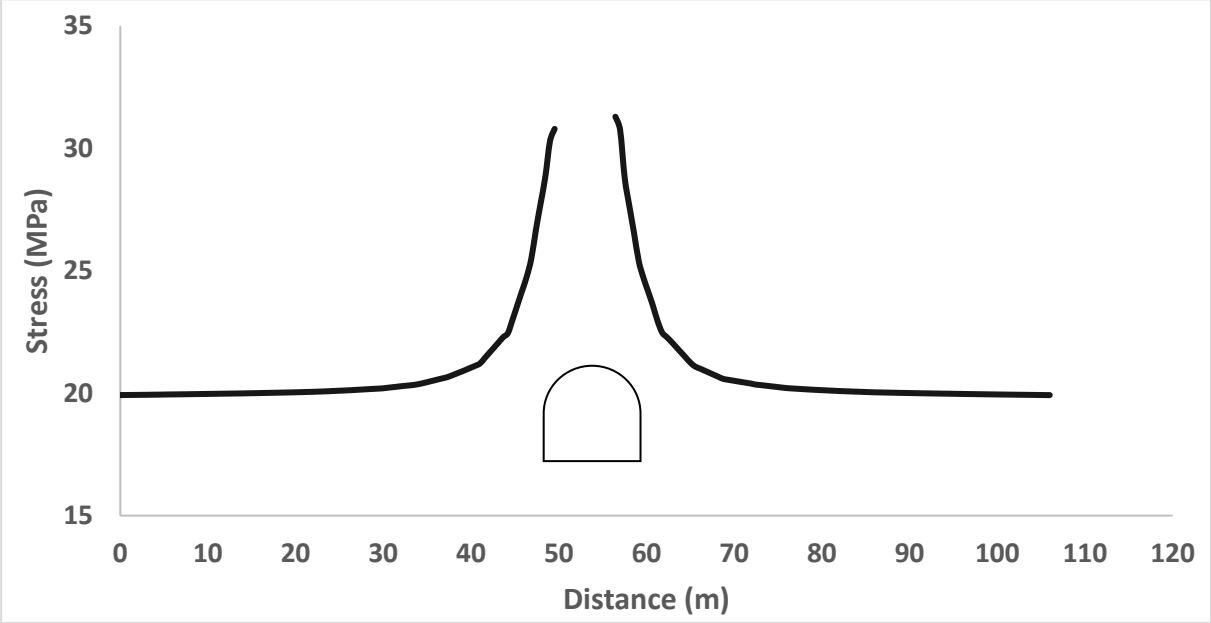

Figure 8. Stress Distribution Around the Decline Shaft

Determination of the plastic zone (Figure 10) and the amount of deformation in the decline shaft (Figure 9) using equations (7) and (8) obtained the following results Table 2:

Table 2. Decline Shaft Deformation Calculation Results

No	Sec	H	σcm/po	dp/do	δi/do
1	1-A	100	0.29	25.57	24.43
2	1-B	100	0.44	19.96	10.33
3	2-A	100	0.62	16.47	5.26
4	2-B	100	0.76	14.64	3.48
5	3-A	100	1.11	11.77	1.62
6	3-B	100	1.60	9.55	0.78
7	4-A	100	1.88	8.73	0.57
8	4-B	100	1.94	8.58	0.53
9	5-A	100	2.10	8.18	0.45
10	5-B	100	2.16	8.07	0.43

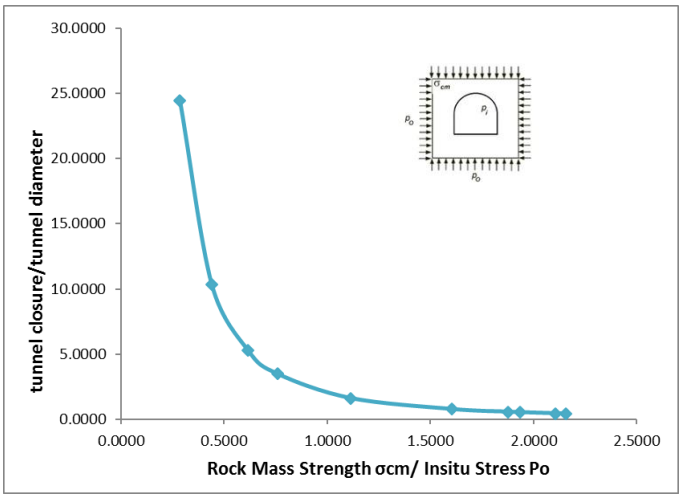

Figure 9. Graph of Decline Shaft Deformation to Insitu Stress

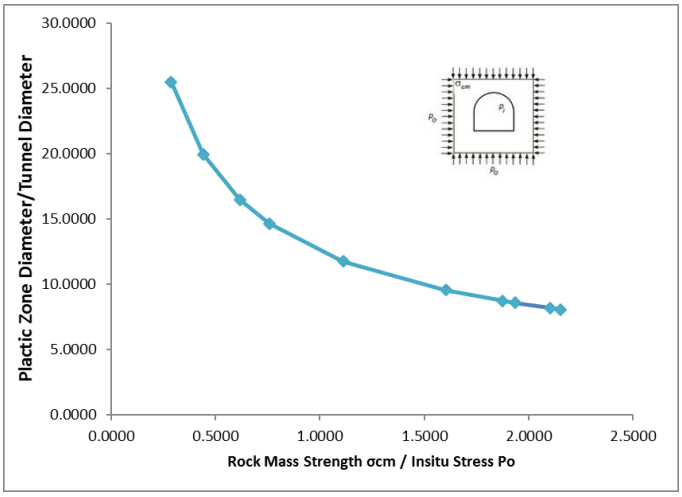

Figure 10. Graph of Plastic Zone to Decline Shaft Diameter

4. Conclusion

The value of stress will experience an increase in both horizontal stress and vertical stress when multiplying occurs. The cause of the increased stress that occurs around the decline shaft is due to the load that was originally borne evenly transferred and redistributed. The results of 2D analysis using the finite element method, the direction of stress redistribution is mostly towards the side wall so that more attention is needed on the side wall so that there is no collapse or lifting of the floor of the incline shaft hole. The maximum stress value is found on the right side of the incline shaft hole of 65.41 MPa. The stress magnitude in the plastic zone is obtained with a value of 25.51 MPa and if the induced stress has a magnitude exceeding the maximum value of the plastic zone there will be instability. Based on the analysis results from the calculation of the decline shaft deformation and the direction of the stress distribution, the recommendation for the support design for weak rocks can be used steel rib with a combination of concrete / shotcrete lining.

References:

[1] Z. T. Bieniawski, *ROCK MECHANICS DESIGN IN MINING AND TUNNELING*. 1984.

[2] R. H. K. Putri, "Coal Pillar Strength Formula in Indonesian coal mines," *J. Earth Mar. Technol.*, 2020, doi: 10.31284/j.jemt.2020.v1i1.1147.

[3] R. H. K. Putri, "Penentuan Lebar Chain Pillar Pada Tambang Batubara Shortwall Mining," *Indones. Min. Prof. J.*, 2020, doi: 10.36986/impj.v2i1.21.

[4] Y. D. Galih C, G. S. Utami, and A. Khanifa, "The Influence of Structural Structures on Slope Stability at PT. Energi Batubara Lestari, South Kalimantan)," *PROMINE*, 2019, doi: 10.33019/promine.v7i1.1059.

[5] M. Cai, P. K. Kaiser, and C. D. Martin, “Quantification of rock mass damage in underground excavations from microseismic event monitoring,” *Int. J. Rock Mech. Min. Sci.*, 2001, doi: 10.1016/S1365-1609(01)00068-5.
[6] A. Zamroni, O. Sugarbo, R. Prastowo, F. R. Widiatmoko, Y. Safii, and R. A. E. Wijaya, “The relationship between Indonesian coal qualities and their geologic histories,” 2020, doi: 10.1063/5.0006836.
[7] S. E. Haryanto, B. Budiarto, A. S. Sari, and F. R. Widiatmoko, “No TKajian Teknis Sistem Penyaliran Tambang Dan Rancangan Sumuran Pada Pit Majapahit PT. Prolindo Cipta Nusantara, Kabupaten Tanah Bumbu, Kalimantan Selatanitle,” in *Prosiding Seminar Nasional Sains dan Teknologi Terapan*, 2019, pp. 539–544.
[8] Y. D. G. Cahyono, “Technical Planning of Ventilation System to Support Development W Undercut in 2021 at PT. Freeport Indonesia Underground Mining,” *J. Earth Mar. Technol.*, 2020, doi: 10.31284/j.jemt.2020.v1i1.1141.
[9] W. E. C. Putri, A. Zamroni, and F. R. Widiatmoko, “PENGARUH AKTIVITAS PERTAMBANGAN TERHADAP NILAI PRODUK DOMESTIK REGIONAL BRUTO DAN EKONOMI MASYARAKAT DI PROVINSI KALIMANTAN TIMUR,” *KURVATEK*, vol. 5, no. 2, pp. 71–76, Dec. 2020, doi: 10.33579/krvtk.v5i2.1854.
[10] B. H. G. Brady and E. T. Brown, *Rock Mechanics for underground mining: Third edition*. 2006.
[11] F. R. Widiatmoko, A. Zamroni, M. A. Siamashari, and A. N. Maulina, “REKAMAN STASIUN GPS SEBAGAI PENDETEKSI PERGERAKAN TEKTONIK, STUDI KASUS: BENCANA TSUNAMI ACEH 26 DESEMBER 2004,” 2019.
[12] E. Hoek and E. T. Brown, “Practical estimates of rock mass strength,” *Int. J. rock Mech. Min. Sci. Geomech. Abstr.*, 1997, doi: 10.1016/S0148-9062(97)00305-7.
[13] E. Hoek and E. T. Brown, “The Hoek–Brown failure criterion and GSI – 2018 edition,” *J. Rock Mech. Geotech. Eng.*, 2019, doi: 10.1016/j.jrmge.2018.08.001.
[14] G. Herget and S. Vongpaisal, “Proceedings of the 6th congress of the International Society for Rock Mechanics, Montreal, 1987. Three volumes.,” *Proc. 6th Congr. Int. Soc. Rock Mech. Montr. 1987. Three Vol.*, 1987.
[15] K. Terzaghi and F. E. Richart, “Stresses in rock about cavities,” *Geotechnique*, 1952, doi: 10.1680/geot.1952.3.2.57.
[16] P. R. Sheorey, “A theory for In Situ stresses in isotropic and transverseley isotropic rock,” *Int. J. Rock Mech. Min. Sci.*, 1994, doi: 10.1016/0148-9062(94)92312-4.
[17] M. Li, J. Zhang, Z. Wu, and K. Sun, “Calculation and monitoring analysis of stress distribution in a coal mine gob filled with waste rock backfill materials,” *Arab. J. Geosci.*, 2019, doi: 10.1007/s12517-019-4584-9.
[18] Z. T. Bieniawski, “Engineering classification of jointed rock masses. discussions of paper by Z.T. Bieniawski, trans. s. afr. instn. civ. engrs. v15, n12, Dec. 1973, and authors reply,” *Int. J. Rock Mech. Min. Sci. Geomech. Abstr.*, 1974, doi: 10.1016/0148-9062(74)92075-0.
[19] J. M. Galvin, *Ground engineering - principles and practices for underground coal mining*. 2016.